JnUJSci

Jagannath University Journal of Science
Volume 09, Number II, December 2022, pp. 64−70
https://jnu.ac.bd/journal/portal/archies/science.jsp
ISSN 2224-1698

Alpha-Nucleus Potentials at 25 MeV

Research Article

Mohammad Ullah, Shuva Saha and M. Nure Alam Abdullah*

Department of Physics, Jagannath University, Dhaka-1100, Bangladesh

Received: 29 November 2022, Accepted: 17 May 2023

ABSTRACT

The elastic scattering of α-particles from the ^{50,52,53}Cr, ^{63,65}Cu, ^{64,66,70}Zn and ^{70,72}Ge targets at 25 MeV are analyzed in terms of the non-monotonic (NM) potentials within the framework of the optical model (OM). The NM potential is a complex potential with a soft repulsive core in its real part bearing the volume integral per nucleon pair around −100 MeV.fm^3. The empirically adjusted imaginary potential is used in conjunction with the real part of the NM potential to reproduce the experimental angular distributions. The derived potentials have been found satisfactory in reproducing the cross sections at 25 MeV for the targets studied in this study. The variation of volume integrals with target mass number has also been studied which can be useful in estimating the volume integral for any isotope at 25 MeV.

Keywords: *Optical model, Non-monotonic potential, Volume integra, Shallow potential*

1. Introduction

Many nuclear phenomena such as elastic scattering, inelastic scattering, transfer reactions, and projectile fragmentation take place when a target nucleus is bombarded with a nucleon or light ions. Different types of projectiles are allowed to collide with the target nucleus, and the interactions are studied using scattering, reaction, and bound state data. Different nuclear potentials are proposed in order to properly explain the experimentally obtained data. Out of a number of potentials, the optical model (OM) potential is often used as it can explain the loss of flux from the incident channel to the outgoing channels. The OM potential is a complex potential which serves as the OM's representation of a nucleus. In the OM's representation the complex potential has two parts: real part and imaginary part. The real part represents elastic scattering while the imaginary part takes into account of non-elastic processes. The scattering and reaction cross sections are obtained from the Schrödinger equation when the OM potential is taken into account as a function of space coordinates and energy of the bombarding particles.

There are two types of OM potentials. The first one is the phenomenological OM potential which is obtained from the direct analysis of the experimental elastic scattering data. The Woods-Saxon (WS) (Woods and Saxon 1954) and squared

*Corresponding author: M. Nure Alam Abdullah
E-mail: abdullah@phy.jnu.ac.bd

WS (SWS) (Delbar *et al.* 1978) potentials are of this type. The other group, which is called microscopic OM potential, is derived from the realistic nucleon-nucleon (N-N) interaction. This group includes the double-folded (DF) (Brandan and Satchler 1997, Satchler and Love 1979) potential and non-monotonic (NM) potential (Tariq *et al.* 1999, Abdullah *et al.* 2005, Billah *et al.* 2005, Hossain *et al.* 2013). The NM potential has its root in the energy-density functional (EDF) formalism of Brueckner, Coon, and Dabrowski (BCD) (Brueckner *et al.* 1968).

The unusual enhancement of cross sections at large angles, commonly known as the anomaly in large scattering angle (ALAS) (Correlli *et al.* 1959, Gruhn and Wall 1966, Bobrowska *et al.* 1969, Eickhoff *et al.* 1975, Trombik *et al.* 1975, Jarczyk *et al.* 1976, Kobos *et al.* 1974), is a dominant feature of the α-induced elastic scattering and non-elastic processes at $E_\alpha \leq 50$ MeV. Corelli *et al.* (1959) first observed the ALAS feature of experimental data on the elastic scattering of α-particles for ^{16}O and ^{32}S targets up to about 50 MeV. Since then, it has been seen to exist for a number of other targets up to ^{48}Ca (Gruhn and Wall 1966, Bobrowska *et al.* 1969, Eickhoff *et al.* 1975, Trombik *et al.* 1975, Jarczyk *et al.* 1976, Kobos *et al.* 1974). At $E_\alpha > 50$ MeV incident energy, the ALAS effect diminishes producing the so-called "rainbow scattering", characterized by a significant decrease in cross sections beyond a particular scattering angle.

The elastic scattering of α-particles on various targets has been shown to be inadequately reproduced by the Woods-Saxon (WS) OM potential, despite the fact that it can successfully explain the nucleon-nucleus elastic scattering (Correlli *et al.* 1959, Gruhn and Wall 1966, Michel *et al.* 1986, Michel *et al.* 1995). The WS potential has been found to be inconsistent in describing the data of Kemper *et al.* (1972) on the elastic scattering of α-particles by ^{27}Al at $E_\alpha = 22.3 - 27.5$ MeV. Some energy points need shallow WS potential while some other energies require deep WS potential to reproduce the experimental angular distributions of α+^{27}Al elastic scattering. McFadden and Satchler (1966) faced the identical problem and had to use a shallow potential to fit the data of Budzanowski *et al.* (1964) at 24.7 MeV incident energy. In addition, the WS potentials failed to describe the α-induced inelastic scattering (Bobrowska *et al.* 1969, Budzanowski *et al.* 1978) and transfer reactions (Bland *et al.* 1980, Jankowski *et al.* 1984, Bao *et al.* 1986, Kajihara *et al.* 1994).

The non-monotonic (NM) type of complex potential (Manngård *et al.* 1989, Tariq *et al.* 1999, Abdullah *et al.* 2003, Abdullah *et al.* 2005, Billah *et al.* 2005, Hossain *et al.* 2013) with a soft repulsive core in its real part, proposed by Malik and his group (Block and Malik 1967, Rickertsen *et al.* 1969, Reichstein and Malik 1971) has been proven to be successful in expaining the elastic scattering of α-particles on various targets. The NM potential can be derived from the EDF theory (Brueckner *et al.* 1968, Reichstein and Malik 1971, Malik and Reichstein 1992) using the sudden approximation and has a volume integral per nucleon pair $J_R/(4A) \approx -100$ MeV.fm^3. Tariq *et al.* (1999) described the α elastic scattering data on ^{28}Si for incident energies between 14.5 and 45.0 MeV, ^{30}Si at 26.6 MeV, and ^{24}Mg at energies between 22.0 and 120.0 MeV by the NM potential. Abdullah *et al.* (2003, 2005) successfully explained the experimental angular distributions of α-particles on ^{27}Al and ^{40,44,48}Ca using the NM type of OM potential. The work of Billah *et al.*(2005) satisfactorily described the observed angular distributions of α+^{58,60,62,64}Ni elastic scattering in terms of the NM potentials. Hossain *et al.* (2013) used NM potentials to reproduce the experimental α+^{90}Zr elastic scattering data in the energy range $15.0 - 141.7$ MeV bombardment energy. In the energy range of $79.5 - 141.1$ MeV, the shallow NM potential also provides a good explanation for the overall structure of the nuclear rainbow scattering for α+^{90}Zr elastic scattering (Hossain *et al.* 2013).

In this present study we examine the α-particle elastic scattering data on ^{50,52,53}Cr, ^{63,65}Cu, ^{64,66,70}Zn and ^{70,72}Ge target nuclei at 25 MeV incident energy. The purpose of the present work also includes to find a relation between the volume integral per nucleon pair for the real part $J_R/(4A)$ at 25 MeV with the target mass number of the nuclei studied in the present work.

2. Non-monotonic Potential

Block and Malik (1967) first formulated the fundamental framework of the NM potential. After that, Rickertsen *et al.* (1969) presented the ^{16}O-^{16}O potential which is NM in nature. In a model of transient nuclear matter, the parameters of this potential were calculated based on the two-nucleon potential. However, using the EDF formalism with sudden approximation, Brueckner *et al.* (1968) precisely determined the potential with a central repulsive core from two-nucleon interaction although it had a numerical inaccuracy. The NM potential is predicted in both sudden and adiabatic approximations, according to the work of Reichstein and Malik (1971). The sudden approximation was comparable to the one used by Rickertsen *et al.* (1969) to fit the ^{16}O+^{16}O elastic scattering data. Later, Haider and Malik (1981) eventually expanded the fit to higher incident energies.

The NM potential can be parameterized by the following forms (Manngård *et al.* 1989, Tariq *et al.* 1999, Abdullah *et al.* 2005, Billah *et al.* 2005, Hossain *et al.* 2013) of real $V_{NM}(r)$ and imaginary $W_{NM}(r)$ terms:

$$V_{NM}(r) = -V_0\left[1+\exp\left(\frac{r-R_0}{a_0}\right)\right]^{-1} + V_1\exp\left[-\left(\frac{r-D_1}{R_1}\right)^2\right] + V_C(r), \quad (1)$$

$$W_{NM}(r) = -W_0\exp\left[-\left(\frac{r}{R_W}\right)^2\right] - W_S\exp\left[-\left(\frac{r-D_S}{R_S}\right)^2\right]. \quad (2)$$

The real potential is made non-monotonic by adding a short-ranged repulsive potential in the second part of the right hand side of Eq. (1) with the attractive first part. Here V_0 is the attractive depth with R_0 and a_0 as the radius parameter and diffuseness parameter respectively; V_1 is the depth of the repulsive component with D_1 and R_1 as the shift parameter and the range parameter. We have used $D_1 = 0$ for unshifted repulsive core in this study. Eq. (2) comprises both volume and surface type in which W_0 and R_W are, respectively, the depth and range parameters of the volume imaginary, and W_S, R_S and D_S are, respectively, the depth, range and shift parameters of the surface imaginary potential.

The Coulomb potential is then given by

$$V_C(r) = \begin{cases} \frac{Z_1Z_2e^2}{2R_c}\left(3-\frac{r^2}{R_c{}^2}\right), & r \le R_c \\ \frac{Z_1Z_2e^2}{r}, & r > R_c\ . \end{cases} \quad (3)$$

Here Z_1 and Z_2 are, respectively, the charges of the projectile and target nucleus. The Coulomb radius R_C in the NM potential is equal to $R_C = R_{\alpha C} + r_C A^{\frac{1}{3}}$, where $r_C = 1.35$ fm and A is the mass number of the target. $R_{\alpha C}$ is linked with the large tail of the α-particle.

3. Analysis and Results

The experimental α+^{50,52,53}Cr, α+^{63,65}Cu, α+^{64,66,70}Zn and α+^{70,72}Ge elastic scattering data at $E_\alpha = 25$ MeV projectile energy are taken from Su and Han (1969). These experimental data are analyzed using the code SFRESCO which incorporates the coupled-channels code FRESCO 2.5 (Thompson 1988). To fit the experimental angular distributions, the chi-square minimization code MINUIT (James and Roos 1975) has been used in conjunction with SFRESCO. A set of parameters is obtained by minimizing the χ^2 defined as

$$\chi^2 = \frac{1}{N}\sum_i\left[\frac{\sigma_{exp}(\Theta_i)-\sigma_{th}(\Theta_i)}{\Delta\sigma_{exp}(\Theta_i)}\right]^2. \quad (4)$$

Here $\sigma_{exp}(\Theta_i)$is the experimental cross section with $\Delta\sigma_{exp}(\Theta_i)$ as its error at the scattering angle Θ_i. $\sigma_{th}(\Theta_i)$ is the cross section calculated using the NM potential by analyzing the data. N is the number of data points for a given projectile α-energy.

Table 1. The NM real potential parameters for the best fits to the α+^{50,52,53}Cr, α+^{63,65}Cu, α+^{64,66,70}Zn and α+^{70}Ge elastic scattering data along with the volume integrals per nucleon pair. V_0 and V_1 are in MeV; R_0, R_1, R_C, a_0 in fm; $J_R/(4A)$ in MeV.fm^3.

Target	V_0	R_0	a_0	V_1	R_1	R_C	$J_R/(4A)$
^{50}Cr	35.96	5.380	0.580	42.24	3.100	10.0	–98.32
^{52}Cr	20.97	9.324	1.500	42.00	0.969		–396.98
^{53}Cr	19.34	9.590	1.250	33.00	2.220		–366.87
^{63}Cu	19.60	10.330	1.162	42.00	0.200		–398.73
^{64}Zn	12.03	7.880	0.700	60.70	2.650		–79.25
^{65}Cu	22.95	6.560	0.864	42.00	1.815		–117.04
^{66}Zn	12.00	8.000	0.767	136.5	2.160		–77.31
^{70}Zn	13.02	6.600	0.800	31.00	2.900		–49.08
^{70}Ge	12.70	6.840	0.700	28.33	2.720		–55.75

In order to analyze the experimental α+^{50,52,53}Cr, α+^{63,65}Cu, α+^{64,66,70}Zn and α+^{70}Ge elastic scattering data at 25 MeV in terms of NM potential, we have used the real potential given in Eq. (1) in conjunction with the imaginary potential given in Eq. (2). The potential parameters are searched in such a way that the obtained NM potential has volume integral $J_R/(4A) \approx -100$ MeV.fm^3, as the NM potential has the volume integral per nucleon pair for the real part typically around -100 MeV.fm^3. The whole experimental data are analyzed using the NM potential with $D_1 = 0$. The potential parameters along with the volume integrals of the real part are tabulated in Table 1. The parameters of the corresponding imaginary potential, volume integrals per nucleon pair and χ^2-values are displayed in Table 2. The value of the Coulomb radius is held fixed as $R_C = 10.0$ fm for all the targets studied in this work. As can be seen from Table 1, ^{52}Cr, ^{53}Cr and ^{63}Cu need inconsistent values of R_0 as well as a_0. Accordingly, the volume integral per nucleon pair, $J_R/(4A)$ for the real part has unusual values as –397.0, –366.9 and –398.7 MeV.fm^3 respectively for these three targets. While the data for ^{50}Cr, ^{64}Zn, ^{65}Cu, ^{66}Zn, ^{70}Zn, and ^{70}Ge targets require the integral values from $J_R/(4A) = -55.75$ to $J_R/(4A) = -117.0$ MeV.fm^3.

Figures 1 displays the fits to the experimental α+^{50,52,53}Cr, α+^{63,65}Cu, α+^{64,66,70}Zn and α+^{70}Ge elastic scattering data at 25 MeV using NM α-nucleus potential. It is observed that there is an excellent agreement between the theoretical predictions obtained from NM potentials and the experimental data which is also reflected from the χ^2-values given in Table 1.

Table 2. The imaginary NM potential parameters for the best fits to the α+^{50,52,53}Cr, α+^{63,65}Cu, α+^{64,66,70}Zn and α+^{70}Ge elastic scattering data along with the volume integrals per nucleon pair and χ^2. W_0 and W_S are in MeV; R_S, R_W, D_S in fm; $J_I/(4A)$ in MeV.fm^3.

Target	W_0	R_W	W_S	D_S	R_S	$J_I/(4A)$	χ^2
^{50}Cr	25.6	1.140	0.43	6.815	1.40	–4.28	2.00
^{52}Cr	5.1	1.868	8.30	5.524	2.88	–91.52	25.1
^{53}Cr	18.0	0.951	6.03	6.680	3.52	–113.38	7.07
^{63}Cu	18.6	1.523	5.70	5.780	5.0	–113.42	5.55
^{64}Zn	13.0	1.234	1.76	10.800	4.365	–65.26	8.20
^{65}Cu	17.7	1.083	1.70	10.160	2.74	–42.56	3.49
^{66}Zn	13.1	1.050	7.41	6.460	1.72	–46.87	17.0
^{70}Zn	6.0	0.800	4.70	4.945	3.16	–34.83	5.91
^{70}Ge	6.8	1.050	4.70	5.150	3.40	–41.19	7.90

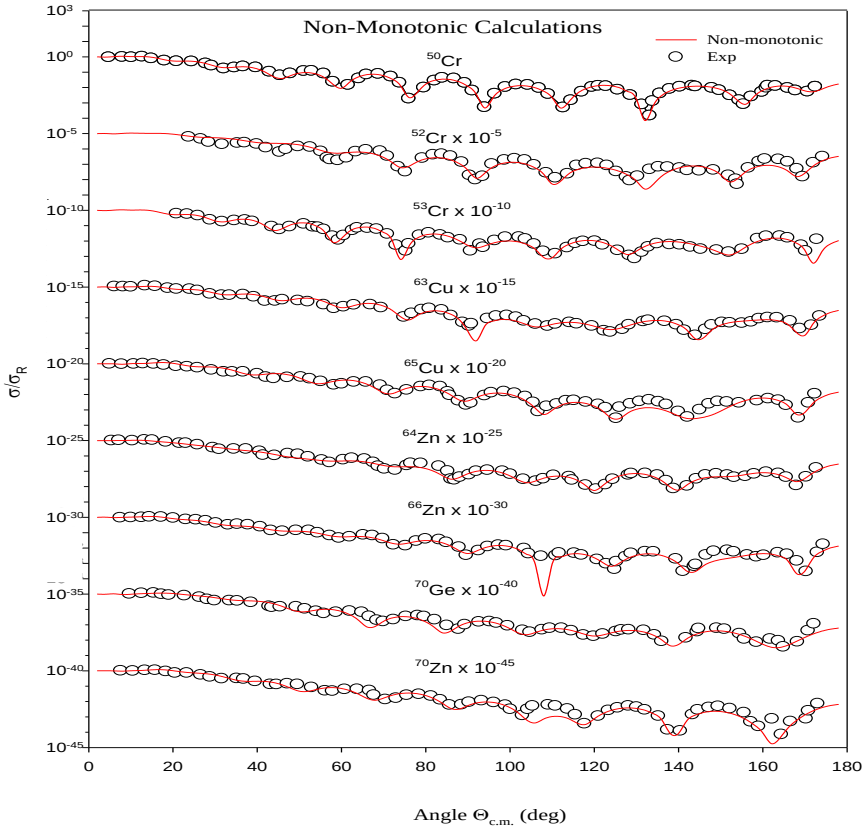

Fig 1. The predicted cross sections using the NM potential are compared to the ratio to Rutherford cross sections for the α+^{50,52,53}Cr, α+^{63,65}Cu, α+^{64,66,70}Zn and α+^{70}Ge elastic scattering data at 25 MeV. The solid curves are the theoretical predictions and the open circles are the experimental data, taken from Su and Han (1969).

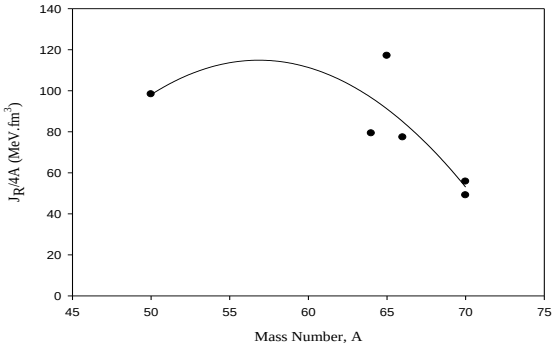

Fig. 2. Variation of $|J_R/(4A)|$ with target mass number at 25 MeV for the real NM α-^{50}Cr, α-^{65}Cu, α-^{64,66,70}Zn and α-^{70}Ge potentials. The solid circles are the integral values and the solid line is the analytical fit to the data.

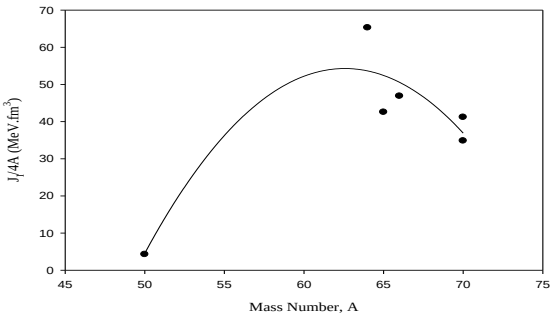

Fig. 3. Variation of $|J_I/(4A)|$ with target mass number at 25 MeV for the imaginary NM α-^{50}Cr, α-^{65}Cu, α-^{64,66,70}Zn and α-^{70}Ge potentials. The solid circles are the integral values and the solid line is the analytical fit to the data.

4. Mass Dependence of Volume Integral

The volume integrals per nucleon pair $J_R/(4A)$ and $J_I/(4A)$, respectively for the real and imaginary parts of the α-^{50,52,53}Cr, α-^{63,65}Cu, α-^{64,66,70}Zn and α-^{70}Ge potentials are plotted in Fig. 2 and Fig. 3 to show the variation of volume integrals with target mass number. Here, the targets ^{52}Cr, ^{53}Cr and ^{63}Cu have been omitted as the volume integrals of the real part for these nuclei are unusually high for the NM potential. For the real part of the NM potential for ^{50}Cr, ^{65}Cu, ^{64,66,70}Zn and ^{70}Ge, the following analytical relation is employed:

$$|J_R/4A| = -1041.5503 + 40.682A - 0.3578\,A^2. \quad (5)$$

Figure 2 displays the variation of volume integral for the real part of the α-^{50}Cr, α-^{65}Cu, α-^{64,66,70}Zn and α-^{70}Ge potentials. The solid circles in this figure are the volume integrals obtained from the analysis of the experimental data and the solid line is the analytical fit using Eq. (5).

For the imaginary volume integrals, the following analytical form has been employed:

$$|J_I/4A| = -1177.7963 + 39.3831A - 0.3147A^2. \quad (6)$$

In Fig. 3, the variation of volume integral for the imaginary part of the α-^{50}Cr, α-^{65}Cu, α-^{64,66,70}Zn and α-^{70}Ge potentials are displayed. The solid circles in this figure are the volume integrals obtained from the analysis of the experimental data and the solid line is the analytical fit using Eq. (6).

5. Discussion and Conclusions

The present study describes the results of analyses of the experimental α elastic scattering cross sections on ^{50,52,53}Cr, ^{63,65}Cu, ^{64,66,70}Zn and ^{70,72}Ge nuclei at 25.0 MeV within the framework of the optical model (OM) using the non-monotonic (NM) potential. The study uses the real part with an unshifted repulsive core *(D_1=0)* to fit the experimental angular distributions of the elastic scattering of α+^{50,52,53}Cr, α+^{63,65}Cu, α+^{64,66,70}Zn, and α+^{70}Ge in terms of the NM potential. Although the NM potential is able to produce good fits to the data (Fig. 1), the volume integral per nucleon pair for the real component shows anomalous values for ^{52,53}Cr, and ^{63}Cu. The volume integrals for these three targets are deep, exceeding 350 MeV.fm^3 (Table 1), which is not what is predicted for the NM potential. However, except for these three targets, the real volume integral has nearly consistent values (Table 1). An attempt has also been made to show the variation of the volume integrals for the real and imaginary parts of the NM potential with target mass numbers which are shown in Figs. 2 and 3.

Mass dependent NM α-nucleus potentials at 25 MeV incident energy are obtained in the present study which can be used to find the nature of α-nucleus potential for a particular target nucleus. Further work needs to be carried out in terms of NM potential with shifted repulsive core ($D_1 \neq 0$) to overcome the discrepancy observed in the volume integrals for the real part of this potential using unshifted repulsive core ($D_1 = 0$).

Acknowledgements

This work is supported by a research grant from Jagannath University, Dhaka, Bangladesh which is thankfully acknowledged.

References

Abdullah MNA, Mahbub MS, Das SK, Tariq ASB, Uddin MA, Basak AK, Sen Gupta HM, Malik FB. 2002. Investigation of α-nucleus interaction in the ^{27}Al(α,α)^{27}Al scattering and ^{27}Al(α,d)^{29}Si reaction. *Eur. Phys. J. A*, 15: 477-486.

Abdullah MNA, Idris AB, Tariq ASB, Islam MS, Das SK, Uddin MA, Mondal AS, Basak AK, Reichstein I, Sen Gupta HM, Malik FB. 2005. Potentials for the α–^{40,44,48}Ca elastic scattering. *Nucl. Phys. A* 760: 40-58.

Bao X, Li S, Wang Y, Yuan R, Huang B, Sun Z. 1986. Influence of α-nucleus ALAS potential on the ^{40}Ca(α,p)^{43}Sc reaction. 1986. *Chin. Phys.* 6: 645-653.

Billah MM, Abdullah MNA, Das SK, Uddin MA, Basak AK, Reichstein I, Sen Gupta HM, Malik FB. Alpha–Ni optical model potentials. *Nucl. Phys. A* 762: 50-81.

Bland LC, Fortune HT, Gorpinich OK, Stryuk YuS, Sheherbin VN, Tokarevskik VV. 1980. Reaction ^{27} Al(α,d)^{29}Si at 27.2 MeV. *Phys. Rev. C* 21: 2227.

Block B, Malik FB. 1967. Effect of the Pauli Principle in O^{16}-O^{16} Elastic Scattering. *Phys. Rev. Lett.* 19:239-242.

Bobrowska A, Budzanowski A, Grotowski K, Jarczyk L, Micek S, Niewodniczański H, Strzalkowski A, Wróbel Z. 1969.Elastic scattering of alpha particles on ^{39}K at E_α = 22.1−28.2 MeV. *Nucl.Phys. A* 126: 361-368.

Brandan ME, Satchler GR. 1997. The interaction between light heavy-ions and what it tells us. *Phys. Rep*.285: 143-243.

Brueckner KA, Coon SA, Dabrowski J. 1968. Nuclear Symmetry Energy. *Phys. Rev.* 168: 1184-1188.

Budzanowski A, Dabrowski H, Freindl L, Grotowski K, Micek S, Planeta R, Strzalkowski A, Bosman M, Leleux P, Macq P, Meulders JP, Pirart C. 1978. Elastic and inelastic scattering of alpha particles on ^{58}Ni and ^{60}Ni in a broad range of energy and angle. *Phys. Rev.* 17: 951-959.

Budzanowski A, Grotowski K, Micek S, Niewodniczanski H, Sliz J, Strzalkowski A, Wojciechowski H. 1964. Elastic scattering of 24.7 MeV alpha particles. *Phys. Lett.*11:74-76.

Correlli JC, Bleuler E, Tendam DJ. 1959. Scattering of 18-Mev Alpha Particles by C^{12}, O^{16}, and S^{32}. *Phys. Rev.* 116: 1184-1193.

Das SK, Tariq ASB, Rahman AFMM, Roy PK, Huda MN, Mondal AS, Basak AK, Sen Gupta HM, Malik FB. 1999. Effect of α-nucleus potential on the ^{27}Al(α,t)^{28}Si reaction. *Phys. Rev. C* 60:044617.

Delbar Th., GrégoireGh, Paic G, Ceuleneer R, Michel F, Vanderpoorten R, Budzanowski R, Dabrowski H, Friendl L, Grotoski K, Micek S, Planeta R, Strzalkowski A, Eberhard A. 1978. Elastic and inelastic scattering of alpha particles from ^{40,44}Ca over a broad range of energies and angles. *Phys. Rev. C* 18: 1237-1248.

Eickhoff H, Frekers D, Lönner H, Poppensieker K, Santo R, Gaul G, Mayer-Böricke C, Turek .1975. Large angle scattering of 100 MeV α-particles from ^{40,44,48}Ca. *Nucl. Phys. A* 252: 333-342.

Gruhn CR, Wall NS. 1966. Large-angle elastic scattering of alpha particles by ^{39}K, ^{40}Ca, ^{42}Ca, ^{44}Ca and ^{50}Ti. *Nucl. Phys.* 81: 161-179.

Hossain S, Billah Masum, Azad MMB, Parvin Farzana, Abdullah MNA, Hasan KM, Uddin MA, Tariq ASB, Basak AK, Reichstein I, Malik FB. 2013. Non-monotonic potential description of alpha–Zr refractive elastic scattering. *J. Phys. G: Nucl. Part. Phys.* 40**:** 102109.

Hossain S, Tariq ASB, Nilima Athoy, Islam MS, Majumder R, Sayed MA, Billah MM, Azad MMB,Uddin MA, Reichstein I, Malik FB, Basak AK. 2015. Dependence of the ^{16}O+^{16}O nuclear potential on nuclear incompressibility. *Phys. Rev. C* 91: 064613.

Jankowski K, Grzeszczuk A, Siemaszko M, Surowiec A, Zipper W, Budzanowski A, Kozik E. 1984. Investigation of the ^{28}Si (α,*p*)^{31}P and ^{28}Si(α, d)^{30}P reactions at E_α = 26 MeV. *Nucl. Phys. A* 426:1-19.

Jarczyk L, Maciuk B, Siemaszko M, Zipper W. 1976. The optical model and distorted-wave analysis of cross- sections for the scattering of the 24-28 MeV alpha particles from ^{28}Si. *Acta Phys. Pol. B* 7: 531-539

Kajihara T, Yasushi Y, Kubo K-I. 1994. The (*p*, α) reaction (I). The left-right asymmetry, the *j*-dependence and the cross-section magnitude. *Nucl. Phys. A* 568: 499-522 (1994).

Kemper KW, Obst AW, White RL. 1972. Elastic Scattering of Alpha Particles from ^{27}A1 in the Energy Range 21-28 MeV. *Phys. Rev. C* 6: 2090-2095.

Kobos M, Brown BA, Lindsay R, Satchler GR. 1984.Folding-model analysis of elastic and inelastic α-particle scattering using a density-dependent force. *Nucl.Phys. A* 425**:** 205-232.

McFadden L, Satchler GR. 1966. Optical- model analysis of the scattering of 24.7 MeV alpha particles.*Nucl.Phys.* 84:177-200.

Malik FB, Reichstein I. *in Clustering Phenomena in Atoms and Nuclei*. Edited by Brenner M, Lönnroth T, Malik FB. p. 126 (Springer-Verlag Berlin, Heidelberg, 1992).

Manngård P, Brenner M, Alam MM, Reichstein I, Malik FB. 1989. Molecular potential and elastic scattering of alpha particles by ^{28}Si from 14 to 28 MeV. *Nucl. Phys. A* 504:130-142.

Michel F, Reidemeister G, Kondo Y. 1995. A potential deduced from low energy ^{16}O(α,α) elastic scattering. *Phys. Rev. C* 51: 3290.

Michel F, Reidemeister G, Ohkubo S. 1986. Evidence for Alpha-Particle Clustering in the ^{44}Ti Nucleus. *Phys. Rev. Lett.* 57: 1215.

Rickertsen L, Block B, Clark JW, Malik FB. 1969. Nuclear Heavy-ion-Heavy- ion Collisions and the Intermediate- State Model. *Phys. Rev. Lett.* 22: 951- 955.

Satchler GR, Love WG. 1979. Folding model potentials from realistic interactions for heavy-ion scattering. *Phys. Rep*. 55: 183-254.

Tariq ASB, Rahman AFMM, Das SK, Mondal AS, Uddin MA, Basak AK, Sen Gupta HM, Malik FB. 1999. Potential description of anomalous large angle scattering of αparticles. *Phys. Rev. C*, 59: 2558-2566.

Trombik G, Eberhardand KA, Eck JS. 1975. Back-angle anomalies in alpha scattering: Inelastic scattering from the calcium isotopes. *Phys. Rev. C* 11**:** 685- 692.

Woods RD, Saxon DS. 1954. Diffuse Surface Optical Model for Nucleon- Nuclei Scattering. *Phys. Rev*. 95: 577- 578.